Key Points:
- ICESat-2 has proven the on-orbit ability of photon-counting lidar for precise and accurate space-based altimetry
- ICESat-2 onboard attitude control systems exceed the ±45 m mission requirement for pointing control
- The satellite is able to follow reference ground tracks to provide repeat measurements within 10 m on average

Correspondence to:
L. Magruder,
magruder@arlut.utexas.edu

ICESat-2 Early Mission Synopsis and Observatory Performance

Lori Magruder[1,2] [ID], Thomas Neumann[3], and Nathan Kurtz[3]

[1]Applied Research Laboratories, University of Texas at Austin, Austin, TX, USA, [2]Department of Aerospace Engineering and Engineering Mechanics, University of Texas at Austin, Austin, TX, USA, [3]NASA Goddard Space Flight Center, Greenbelt, MD, USA

Abstract The Advanced Topographic Laser Altimetry System (ATLAS) onboard the NASA Ice, Cloud, and land Elevation Satellite-2 (ICESat-2) is the newest Earth observing satellite for global elevation studies. The primary objectives for ICESat-2 follow the objectives of its predecessor, ICESat and also focus on providing cryospheric measurements to determine ice sheet mass balance, and monitor both sea ice thickness and extent. However, the global observations support secondary science objectives as well such as biomass estimation, inland water elevation, sea state height and aerosol concentrations. Since launch of ICESat-2, ATLAS has collected more than a trillion measurements. This study provides a mission overview, a description of the operational components that enable the altimeter products for science, on-orbit observatory performance, and assessment of the spacecraft attitude control systems that enable repeat measurements to within 10 m and pointing control within ±45 m. These metrics should be considered for ground-based validation campaigns or science investigations.

Plain Language Summary Space-based remote sensing provides an unequaled point of view for observing changes on Earth's surface. Collecting precise elevation data from this perspective with modern measurement technology holds promise for a wide range of science disciplines given the coverage over all surface types (e.g., land ice, sea ice, inland water, ocean, and vegetation). Over time this high quality data can not only reveal global elevations but elevation change in those regions with repeat measurements. ICESat-2 carries a state-of-the-art laser ranging system for accurate elevation measurements and utilizes onboard instrumentation and databases to help control the laser pointing enabling repeat measurements and individual geodetic (latitude and longitude) points of interest. The repeat measurements are critical for looking at elevation change over time, while the collection of elevations over specific locations on the Earth enable studies for science and validation efforts. ICESat-2 has been on-orbit for over two years and has collected nearly a trillion measurements. Evaluation of the repeat measurements over time indicate the satellite can point to within 10 m while the ability to collect a measurement of a single position on the surface is within the mission specification of ±45 m.

1. ICESat-2 Science and the ATLAS Instrument

Understanding the state of the Earth's Polar Regions is a key component of understanding Earth's dynamic climate (Meredith et al., 2019). Observations of the cryosphere are required to quantify changes, observe trends, and contribute to improvements of predictive models for both the present climate and future change (e.g., National Research Council, 2012). Elevation measurements facilitate these studies and from the vantage point of space satellites provide broad coverage of both the Arctic and Antarctic regions but also create an opportunity to collect global heights for a multitude of additional studies over a broad range of scientific disciplines.

Laser altimetry is a proven technology for elevation measurements from airborne and space-based platforms. The Ice, Cloud, and land Elevation Satellite (ICESat) was operational from 2003 to 2009 and collected climate-critical elevation measurements with the dedicated onboard altimeter, the Geoscience Laser Altimeter System (GLAS; Schutz et al., 2005). When ICESat was decommissioned, the successor was already in development. This next mission would continue the time series of elevation change begun by ICESat and extended through large-scale airborne measurements from NASA's Operation IceBridge (Koenig et al., 2010). ICESat-2, similarly to ICESat, was designated to carry a single laser altimeter instrument but

had the advantage of lessons learned from the predecessor. These lessons included generating contiguous along-track measurements (instead of ICESat's spot to spot separation of 172 m) and generating smaller multiple footprints (rather than ICESat's single, 70 m diameter footprint) to simplify feature resolution and the separation of surface slope from true elevation change when repeat measurements are collected. The ICESat-2 design is summarized by Markus et al. (2017) and includes multiple beams, smaller laser footprint diameter, and contiguous along-track coverage to recover finer surface features through higher laser repetition rates. ATLAS (Advanced Topographic Laser Altimeter System) is the photon-counting lidar instrument developed at NASA Goddard Space Flight Center for ICESat-2. A comprehensive description of the instrument design and operational implementation is provided by Neumann et al. (2019).

The ICESat-2 mission utilizes an orbit with a 92° inclination for global coverage from 88° South to 88° North latitudes. The orbit is non-sun-synchronous, but frozen (e.g., perigee is prescribed to a specific latitude) with an average altitude of 496 km. The orbital parameters create a repeat measurement cycle of 91 days, with 1387 unique orbits that result in equal longitudinal distribution of ground track coverage. Repeat measurements are critical to quantifying ice sheet elevation change but an off-pointing strategy over successive 91-days cycles is used over the mid-latitudes to create a higher coverage density of measurements in support of terrestrial ecology, bathymetry, and hydrological applications. A diffractive optical element separates the single ATLAS beam into 6 beams, organized into 3 beam pairs (deemed left, nadir. and right pairs). The left and right pairs are both 3.3 km apart from the nadir-most pair in the across-track direction while a small 2° yaw offset in the satellite attitude creates a 90 m across-track separation between the beams within a single pair. Within each pair one beam is 4X the energy of the other, allowing for a greater dynamic range when collecting useful data over a wide range of surface reflectivity. Each laser footprint on the surface is ~11 m in diameter (Magruder, Brunt, Neumann, et al., 2020) with a center-to-center separation of 0.7 m in the along-track direction.

ATLAS range measurements are used in concert with supporting instrumentation onboard the ICESat-2 observatory to provide precise and accurate geolocated elevations. A critical component of the altimetry process is the laser pointing determination. To eliminate geolocation errors due to misalignments among the components used in geolocation determination, a specialized co-axial instrument was designed for zenith collection of stars and nadir collection of the 6 laser beam positions relative to the instrument coordinate system. This instrument is the Laser Reference System (LRS) and was developed specifically to mitigate misalignment issues previously experienced with ICESat. The observed star field observations are designed to combine with a 4-sense axis hemispherical gyro to produce data streams for precision pointing determination of each laser beam at the ICESat-2 10 kHz laser pulse repetition frequency (Bae et al., 2018). The orbit determination solution is derived from the ICESat-2 onboard GPS receivers (Luthcke et al., 2021). The pointing and orbit position data are combined with the ATLAS photon times of flight to produce geodetic positions and elevations for each detected photon. These science data are telemetered to two primary ground stations for processing, in addition to observatory data for health and instrument monitoring. The ground processing system first converts the telemetry to engineering units and combines the time of flight, pointing, and orbit data streams to produce a geolocated point cloud, the Global Geolocated Photons Level 2 product-ATL03 (Neumann et al., 2019). Higher level along-track data products are surface type specific in order to optimize the elevation retrievals with respect to the surface feature characteristics and reflectivity (e.g., oceans, land, sea ice, land ice, and inland water).

We review the on-orbit performance of the ICESat-2 observatory in terms of its on-orbit pointing control and stability, along with the current data recovery metrics in this article. The initial on-orbit performance of ATLAS is described in companion papers (Bae et al., 2021, Luthcke et al., 2021) and in a study by Martino et al. (2019).

2. On-Orbit Observatory Performance and Achievements

The observatory launched from Vandenberg Air Force Base, CA on September 15, 2018. The mission's frozen orbit has an eccentricity of 0.0013 with optimal repeat orbit conditions (near sub-cycle repeats at 29 and 62 days for monthly sampling of the polar sea ice cover) and minimum altitude variation among each orbit pass (between 490 and 512 km). On-orbit operations support orbital parameter adjustments to meet a

requirement of maintaining the ICESat-2 sub-satellite point on the surface to within ±800 m of its nominal value and correcting for drag induced inclination drift. To promote repeat-track data collection, the observatory points the boresight of the ATLAS telescope at the desired target: Along the repeated tracks in the polar regions and/or off-pointing in the mid-latitudes to densify the track coverage. As such, variation in the sub-satellite point leads to variation of the laser beam angle of incidence with respect to Earth. The orbit is critical to collecting the science observations as are the systems that help provide the onboard attitude to achieve repeat measurements and optimized spatial coverage. Here, we evaluate the attitude determination used in the onboard Attitude Control Systems (ACS), as well as the precision attitude determination used in the geolocation process.

2.1. Attitude Control System Performance

The spacecraft ACS is tasked with ensuring ATLAS measurements follow prescribed tracks to satisfy repeat measurements. The Reference Ground Tracks (RGT) provide this targeted path along each orbit in the repeat cycle, and is an imaginary line between the middle beam pair: Ground-track 2 left and ground-track 2 right (GT2l and GT2r). RGT #1 starts ascending just west of Greenwich. The ACS uses the onboard Sodern Star Tracker (SST), with the SSIRU (Scalable Space Inertial Reference Unit) gyro measurements to derive a rapid attitude solution within an instrument frame alignment feedback loop to maintain the RGT prescribed positions. The tracking is based on an onboard calibrated table of the empirical solution for tracking that relates the observatory orbit position to the RGT. Also critical to RGT tracking is the alignment of the ATLAS receiver telescope field of view to the RGT. This alignment is accomplished using four reference spots measured in the LRS laser-side focal plane as part of the Telescope Alignment Monitoring System (TAMS). These TAMS reference spots support fine pointing generation by linking the ATLAS telescope pointing direction in the instrument coordinate frame to the main observatory frame and onboard quaternions from the star tracker. The observatory is required to be able to point the ATLAS telescope to the RGTs to within ±45 m to ensure that successive passes on a given RGT have some measure of overlap for each 90 m-spaced beam pair.

The original ACS calibration table onboard was based on pre-launch ATLAS and observatory alignment measurements and did not include the impact of the zero gravity environment or time-varying pointing and alignment bias calibrations that have significant impact on the quality of the RGT pointing control. These variations were modeled once on-orbit but are also dependent on the solar angle that governs the thermal contributions to instrument misalignment over time and orbit angle. The full angle impact on the attitude determination retrievals for pointing control is not known until calibrations can be estimated throughout a complete solar cycle. Static and time varying biases for instrument pointing, ranging and timing are determined through observatory maneuvers and dynamic crossovers (Luthcke et al., 2005). These maneuvers happen regularly and are performed primarily over the ocean over a partial orbit (ocean scans: OS) or during a complete orbit on a weekly cadence (round-the-world scans: RTW). The calibrations derived from both the OS and the RTW scans maneuver analysis facilitated updates to the empirical solutions in the onboard ACS calibration tables.

Early on-orbit RGT tracking placed along-track profiles ~4 km across-track distance from the RGTs on average indicating that the most significant pointing bias was related to the spacecraft roll axis. The initial pointing model (pitch and roll biases) soon after launch was derived solely from the scan maneuvers while the range biases were determined through short-period measurement crossovers. These data were the basis of interval updates to the ACS onboard calibration table for continual improvements to the RGT tracking accuracy. By March 2019 the accumulation of results from the scan maneuvers and crossover analysis in addition to the collection of time-varying parameterization created an ACS calibration table that allowed for RGT tracking control to within ~10 m (1σ) horizontally over ~1,700 km segment lengths (Luthcke et al., 2021).

In addition to RGT tracking, the observatory also has the ability to target specific coordinates provided within the instrument command file to collect measurements at a dedicated geographical location. These instances are deemed Targets of Opportunity (TOOs), and are particularly important for the ground-based validation studies that benefit from increasing collection opportunities from RGTs in close proximity (Magruder, Brunt, & Alonzo, 2020). This capability allows the observatory to rotate about the main reference

frame, primarily in the roll direction, up to 5° off-nadir (equivalent of 43 km horizontal distance from the sub-satellite point). Based on the observed performance for the pointing at White Sands Missile Range (WSMR) in New Mexico for validation purposes (Magruder, Brunt, Neumann, et al., 2020), the TOO pointing control is better than the prescribed ±45 m, with a variability observed between 12 – 40 m horizontal distance from the submitted target coordinates. Certainly, there are many factors that impact pointing control such as observatory orientation and off-nadir angle but the observed performance is well within the mission requirements and indicates the ability to repeat data collection over a single point, or along an RGT.

As discussed previously, the ICESat-2 observatory routinely points to RGTs over the polar regions to enable change detection measurements. However, over the mid-latitudes the observatory performs an "off-pointing" strategy to increase the spatial extent of the observations in support of land and vegetation objectives (Markus et al., 2017). The strategy for improving coverage will create a uniform distribution of global measurements over the course of 2 years, or 8 RGT cycles, after nominal pointing to the RGTs began in April 2019. As such, we expect to complete this mapping activity in mid-2021.

2.2. Precision Pointing Determination

The precision pointing determination (PPD) process supporting the final ATL03 geolocation solutions also uses the star centroids for attitude determination and the data from the SSIRU gyro (Bae et al., 2018). Originally, the LRS stellar-side was to support PPD given its coaxial design to closely tie the laser vectors with the star field observations. However, once on-orbit the LRS stellar-side indicated anomalous behavior and the attitude determination process transitioned to the SST star trackers that also support ACS related operations. The PPD process goes through a rigorous Extended Kalman Filter (EKF) to estimate errors associated with the quaternions derived from the SST star centroids, and the gyro input scale, misalignment, and bias errors (for yaw, pitch and roll) (Bae & Webb, 2017). The gyro related errors/bias are often difficult to observe during normal observatory operations, but are recovered during the variability within angular motion of the OS maneuvers described previously. The output of the EKF provides the spacecraft precision attitude determination (PAD). The LRS laser-side data determines the position of each of the six laser centroids and the relative pointing vectors similar to its role in the ACS (Bae et al., 2018, 2019, 2021). Correlation of the pointing vectors with the PAD solutions produces the PPD product to be combined with Precision Orbit Determination (Luthcke et al., 2019) to enable geolocation of each detected photon.

The photon geolocation assigns a geodetic position for the laser bounce point on the surface of the Earth (Luthcke et al., 2019). That is, each photon (signal or noise) is attributed to a single laser shot and will be positioned at the calculated centroid of the footprint with the measured elevation regardless of where the photon was reflected within the spatial extent of the laser footprint on the surface. As such, resolution of independent objects occurring within a laser footprint will be vertically resolvable if the elevation difference is more than the elevation precision or ~10 cm (Brunt et al., 2019) but the horizontal resolution is limited by the diameter of the footprint itself. Given the 6.5 m mission requirement for geolocation knowledge, several studies have confirmed the uncertainty of the Release 003 ATL03 data to be within 4 m horizontally and 10 cm vertically (Magruder, Brunt, Neumann, et al., 2020; Luthcke et al., 2021). This is a generalized assessment considering observation variability relative to different orbit angles and length scales, but most validation methods of the geolocation quality provide similar results.

During nominal pointing (either RGT pointing in the polar regions, or off-pointing in the mid-latitudes), the observatory pointing is not perfectly stable. As shown in Figure 1, the observatory pointing (and location of data on the Earth) exhibits both short- and long-frequency variation. When the solar array is orthogonal to the spacecraft direction of motion, the motor that keeps the solar array optimally aligned with the sun causes high frequency motion on the satellite as seen in the onboard gyro rates and subsequent PAD solution (Figure 1a). This motion results in ~meter scale resonance in the across-track direction, as shown in Figure 1b. In Figure 1c, the low frequency, ~10s of meters level frequency of deviation relative to the RGT is mainly due to thermal variations within the observatory that cause time varying misalignments among the instrumentation. We note that in both panels Figure 1b and 1c, the observatory pointing stability is much better than ±45m.
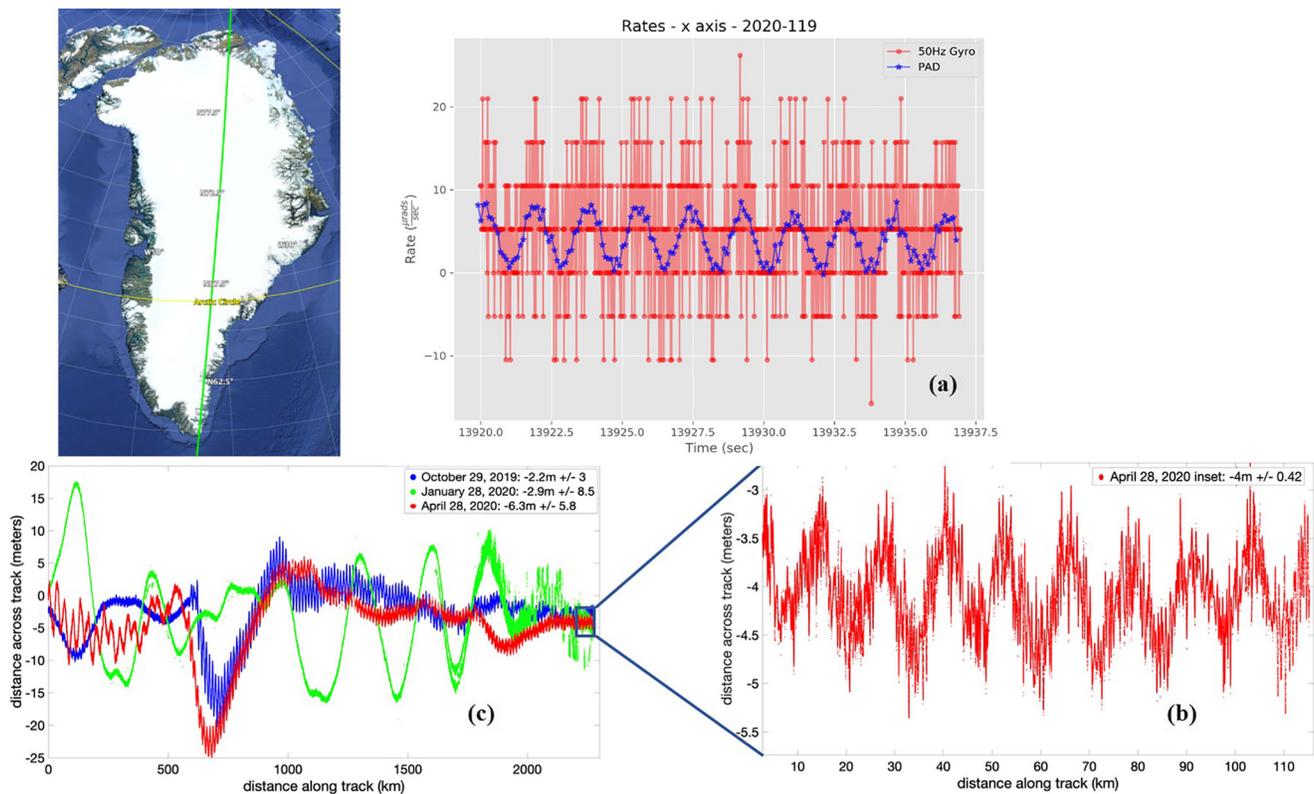
Figure 1. (a) High frequency motion on the satellite from the onboard gyro data and resulting PAD solution due to solar panel motion. (b) This motion results in across-track variation while tracking the RGT while lower frequency motion (c) across-track is a result of thermal variations at longer length scales. PAD, precision attitude determination.

When pointing at TOOs, the observatory uses the same components to determine attitude, but applies a temporary bias to the RGT pointing target. Upon application of this temporary pointing bias, the spacecraft activates reaction wheels to roll to the intended geodetic target. On-orbit data show that this roll takes ~25 s (or ~175 km in ground-track distance) for a 5-degree off-point. This is followed by a 90-s period (or ~630 km of ground-track distance) to allow the spacecraft pointing to stabilize. The TOO location occurs mid-way through this period, by design. After passing the TOO, the temporary bias in the ACS expires, and the observatory transitions back to nominal pointing over the next ~25 s. At large scale, the ground track associated with the TOO appears to progress smoothly and linearly. However, a detailed examination of data locations (Figure 2) reveals the underlying high frequency observatory pointing jitter of several meters in the across-track direction, and low-frequency variation due to the same influences (thermal and solar panel orientation) that is observed during RGT tracking. We note that the high-frequency jitter is smaller than the ATLAS footprint diameter, which means that the observatory is generally able to reliably illuminate small targets (Magruder, Brunt, Neumann, et al., 2020) during TOOs.

3. ICESat-2 Data Products Status and Availability

Algorithm development for the ICESat-2 mission data products began during pre-launch studies. Given the new technology of photon-counting lidar, the expected data characteristics and challenges of making data products to meet the science requirements were essentially unknown. In response to the need for understanding both the photon-counting technology and the potential data quality, the ICESat-2 project developed an engineering testbed system called the Multiple Altimeter Beam Experimental Lidar (MABEL) (McGill et al., 2013). MABEL was configured as an airborne multiple beam, dual frequency lidar with a detection modality sensitive to single photons. It was designed to fly at relatively high altitudes (~20 km) from
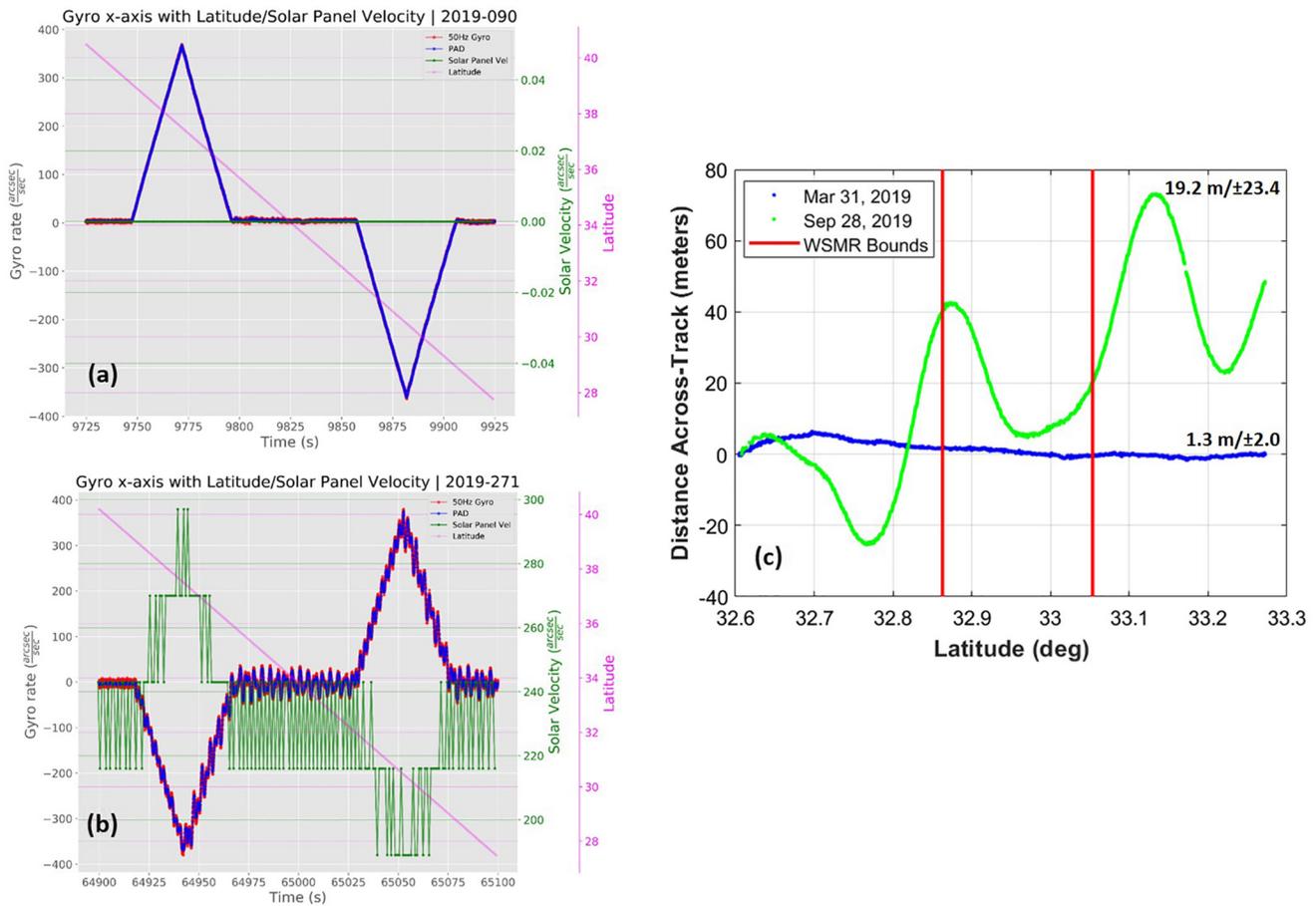
Figure 2. (a) TOO motion when the solar panel is parallel to the direction of motion with corresponding panel velocity and gyro rates as it illuminates ~34° latitude at White Sands Missile Range (WSMR). (b) Is the same TOO with the solar panel in perpendicular orientation. (c) Is the across-track distance for each of the TOOs (March 31, 2019– Day of Year 90, and September 28, 2019–Day of Year 271). TOO, Targets of Opportunity.

the ER-2 platform. Over many test flights in disparate biomes, MABEL provided representative data to the mission science team to use as a proxy to develop initial data product algorithms.

Each of the mission data products uses the prefix of "ATL" and a numerical value that represents a product. The ATL02 product contains all of the instrument and spacecraft measurements used to determine the altimetry foundational information (range, orbital position, and attitude) in addition to the satellite health telemetry. These foundational solutions are combined to create the ICESat-2 Level 2a ATL03 product, the Global Geolocated Photon product (Neumann et al., 2019). The atmosphere uncalibrated backscatter measurements (ATL04) provide quantitative calibration coefficients for the polar regions. ATL03 and ATL04 data are the inputs to each of the higher Level 3a along-track products that are specified relative to the type of surface. That is, land ice (ATL06) (Smith, 2018), sea ice (ATL07) (Kwok et al., 2020), land/vegetation (ATL08) (Neuenschwander et al., 2020), calibrated atmospheric backscatter/cloud characteristic (ATL09) (Palm et al., 2020), ocean (ATL12) (Morison et al., 2020), and inland water (ATL13) (Jasinski et al., 2020).

The vertical telemetry window for the atmospheric data is 15 km, it spans −1 to14 km with respect to the ellipsoid. The vertical telemetry window width for photon-based surface altimetry is variable and depends largely on the type of surface and expected topographic relief for every geographical location. These widths are established via onboard databases (Leigh et al., 2014) once the surface signal is identified through the receiver algorithms (McGarry et al., 2020). The telemetry band can change every 200 shots or 0.05 s (140 m along track). In the presence of significant cloud cover reflections that are misinterpreted as surface echoes, the telemetry band is centered on the cloud top. In these instances the telemetry window may not include

the surface and often causes discontinuous vertical windows. Certainly, in those situations where the true surface return does not exist within ATL03, any subsequent products will also lack accurate elevations.

Another issue noted for ATL03 is the inclusion of an arc of photons beneath the apparent surface signal. The arc actually is comprised of the ATLAS Transmitter Echo Path (TEP) photons, where the system samples a portion of the outgoing laser beam for two of the strong beams (Neumann et al., 2019). These TEP photons are telemetered separately under some circumstances and are used to evaluate the ATLAS on-orbit performance but are omitted from further processing for elevation retrievals within the higher-level, along-track products. Although this is the intent, it is extremely difficult to exclude TEP photons from signal processing when these photons intersect the ground surface elevations and confuse the true surface returns from those of the TEP system. However, there is an ATL03 parameter flag that indicates which signal photons might be attributed to the TEP and assist with further signal filtering downstream.

As with many lidar systems, in some conditions the detector response is observable within the measured point cloud. For ATLAS and the ATL03 product, system impulse response artifacts are most notable over flat, reflective surfaces and appear as one or two parallel surfaces at the distance of ~2.3 and ~4.2 m below the primary returns, similar to detector "ringing" or after pulsing. Although these artifact surfaces are 1/1000 of the energy level of the true surface, they often appear quite prominently particularly for still, open water (Martino et al., 2020). They are best viewed by aggregating data along-track and removing any surface topography. Similar to these data artifacts due to detector response are those from detector saturation. Saturation frequently happens over flat, reflective surfaces where the laser reflections have minimal pulse spreading and signal losses. The returning signal level, in this scenario, often exceeds normal operational detection thresholds which disables subsequent detections until the detector can reset. In ATLAS, this condition happens when 16 or more photons per shot are returned for strong beams, and 4 or more photons per shot are returned for weak beams. Photons incident on the receiver during this "dead time" will not be detected, until the dead time has passed. Further incident photons will be have elevations differences corresponding to the dead time (3.2 ns; Neumann et al., 2019) and create below surface horizons spaced by ~0.5 m for each occurrence.

All of the Level 3a algorithms were implemented before launch and optimization began once the on-orbit operations moved into science mode and data began flowing routinely. As with most algorithms that support new technology, the initial development was limited without real data. Although MABEL data provided a starting point for the processing algorithms, many changes were made once ATLAS data was in hand. The realistic radiometry, noise characteristics and receiver performance warranted adjustments to every product. Following the initial 60 days calibration period and several months of data analysis, the first of the data products were released to the public in May 2019 as release 001 (r001). As of this writing, r003 is the most recent release available, all provided through the National Snow and Ice Data Center (www.nsidc.org). Additional releases are planned on a ~six month cadence as corrections and calibrations are better known and small adjustments in the data algorithms are implemented. Additionally, as more data is acquired, gridded products (Level 3b) will be generated and released.

To date, ICESat-2 has collected more than a trillion measurements since science operations began October 14, 2018. The data acquisition has been continuous except ~2 weeks in July 2019 where the observatory went into safe mode. Safe mode occurs when the onboard telemetry monitoring system detects a fault or out-of-limit value and the observatory powers down all instruments not critical to base-level satellite health, and the solar array tracks the sun. In July 2019, a threshold violation of potentiometer voltage levels occurred during a solar array orientation change from airplane mode (array aligned perpendicular to the direction of motion) to sailboat mode (array aligned along the direction of motion). Once the cause was determined, the satellite systems and onboard instruments were again powered up and returned to science operations. Smaller gaps in data acquisition are frequent during the mission lifetime but never exceed ~4 h length and are commonly less than 10 min per instance. These gaps are attributed to time periods when the satellite performs drag make up maneuvers, or when the laser is put in "arm" mode to avoid illuminating other space-based sensors in near proximity. Over the current mission lifetime ICESat-2 has an on-orbit total of 15,000 h of science data collection, and only 121 h of total data gaps, or ~99% data recovery.

4. Summary

Since the start of the initial mission development in 2007, the ICESat-2 mission has reached several milestones including technical solutions, implementation and on-orbit success. The mission has successfully demonstrated new technology of space-based photon-counting lidar that to date has collected more than a trillion measurements and has proven to support a broad spectrum of science applications. Through pre-launch and post-launch analysis the satellite is able to maintain RGT tracking to 10 m (1σ) for the 1387 orbits in the seasonal repeat cycle and holds the capability for off-nadir measurement strategies with better than ±45 m pointing control. This level of pointing control should be considered when designing experiments or conducting validation activities. For example, for some applications, variation in repeat-pointing ability may be more important (e.g., seasonal snow estimation in rugged terrain) or less important (studies of relatively homogenous ice sheet surfaces). The ICESat-2 geolocated photons show a horizontal position accuracy of 3.6 m (1σ) over both long length scales and through local validation, and a vertical accuracy of better than 10 cm. The operational requirements of the mission have been met to date and measurements satisfy the science objectives of the mission for ice sheet change detection, sea ice freeboard and vegetation mapping.

Data Availability Statement

Data used in this study is compliant with FAIR data standards and publically available/archived at National Snow and Ice Data Center: https://doi.org/10.5067/ATLAS/ATL03.003 (Neumann et al., 2020) and https://doi.org/10.5067/ATLAS/ATL02.003 (Martino, Bock, et al., 2020).

References

Bae, S., Helgeson, B., James, M., Magruder, L., Sipps, J., Luthcke, S., & Thomas, T. (2021). Performance of ICESat-2 precision pointing determination. *Earth and Space Science*, *8*, (4), e2020EA001478.

Bae, S., Helgeson, B., James, M., & Sipps, J. (2019). ICESat-2 precision pointing determination, American Astronautical Society. AAS Paper, 19–777.

Bae, S., Magruder, L., Smith, N., & Schutz, B. (2018). ICESat-2 Algorithm Theoretical Basis Document for Precision Pointing Determination Version 2.0, ICESat-2-SIPS-SPEC-1595.

Bae, S., & Webb, C. E. (2017). Precision attitude determination with an extended Kalman filter to measure ice-sheet elevation. *Journal of Guidance, Control, and Dynamics*, *40*(9), 2335–2340. https://doi.org/10.2514/1.G002715

Brunt, K. M., Neumann, T. A., & Smith, B. E. (2019). Assessment of ICESat-2 ice sheet surface heights, based on comparisons over the interior of the Antarctic ice sheet. *Geophysical Research Letters*, *46*(22), 13072–13078. https://doi.org/10.1029/2019GL084886

Jasinski, M., Stoll, J., Hancock, D., Robbins, J., Nattala, J., Pavelsky, T., et al. (2020). Algorithm theoretical basis document (ATBD) for Inland water data products ATL13 version 003, ICESat-2 scientific computing facility. https://doi.org/10.5067/L870NVUK02YA

Koenig, L., Martin, S., Studinger, M., & Sonntag, J. (2010). Polar airborne observations fill gap in satellite data. *Eos Transactions on AGU*, *91*(38), 333–334. https://doi.org/10.1029/2010eo380002

Kwok, R., Cunningham, G. F., Hancock, D., Ivanoff, A., & Wimert, J. (2020). Algorithm theoretical basis document (ATBD) for sea ice products, ICESat-2 scientific computing facility. Retrieved from https://icesat-2-scf.gsfc.nasa.gov/atbd_docs

Leigh, H. W., Magruder, L. A., Carabajal, C. C., Saba, J. L., & McGarry, J. (2014). Development of onboard digital elevation and relief databases for ICESat-2. *IEEE Transactions on Geoscience and Remote Sensing*, *53*(4).

Luthcke, S. B., Pennington, T., Rebold, T., & Thomas, T. (2019). Algorithm theoretical basis document (ATBD) for ATL03g ICESat-2 receive photon geolocation, ICESat-2 scientific computing facility. Retrieved from https://icesat-2.gsfc.nasa.gov/sites/default/files/page_files/ICESat2_ATL03g_ATBD_r002.pdf

Luthcke, S. B., Rowlands, D. D., Williams, T. A., & Sirota, M. (2005). Reduction of ICESat systematic geolocation errors and the impact on ice sheet elevation change detection. *Geophysical Research Letters*, *32*, L21S05. https://doi.org/10.1029/2005GL023689

Luthcke, S. B., Thomas, T. C., Pennington, T. A., Rebold, T. W., Nicholas, J. B., Rowlands, D. D., et al. (2021). ICESat-2 pointing calibration and geolocation performance. *Earth and Space Science*, e2020EA001494.

Magruder, L. A., Brunt, K. M., & Alonzo, M. (2020). Early ICESat-2 on-orbit geolocation validation using ground-based corner cube retro-reflectors. *Remote Sensing*, *12*(21), 3653. https://doi.org/10.3390/rs12213653

Magruder, L. A., Brunt, K. M., Neumann, T., Klotz, B., & Alonzo, M. (2020). Passive ground-based optical techniques for monitoring the on-orbit ICESat-2 altimeter geolocation and footprint diameter. *Earth and Space Science*. https://doi.org/10.1002/essoar.10504571.1

Markus, T., Martino, T. A., Abdalati, W., Brunt, K., Csatho, B., Farrell, S., et al. (2017). The Ice, Cloud, and land Elevation Satellite-2 (ICESat-2): Science requirements, concept, and implementation. *Remote Sensing of Environment*, *190*, 260–273. https://doi.org/10.1016/j.rse.2016.12.029

Martino, A., Fields, C., & Ramos-Izquierdo, L. (2020). ICESat-2/ATLAS Instrument Linear System Impulse Response. *Earth and Space Science*, https://doi.org/10.1002/essoar.10504651.1

Martino, A. J., Bock, M. R., Gosmeyer, C., Field, C., Neumann, T. A., Hancock, D., et al. (2020). *ATLAS/ICESat-2 L1B converted telemetry data, Version 3*. NASA National Snow and Ice Data Center Distributed Active Archive Center. https://doi.org/10.5067/ATLAS/ATL02.003

Martino, A. J., Neumann, T. A., Kurtz, N. T., & McLennan, D. (2019). ICESat-2 mission overview and early performance. Proceedings of SPIE 11151, Sensors, Systems and Next-Generation Satellites XXIII, 111510C. https://doi.org/10.1117/12534938

McGarry, J., Carabajal, C. C., Saba, J. L., Reese, A. R., Holland, S. T., Palm, S. P., et al. (2020). ICESat-2/ATLAS onboard flight science receiver algorithms: Purpose, process and performance. *Earth and Space Science.* https://doi.org/10.1002/essoar.10502982

McGill, M., Markus, T., Scott, V. S., & Neumann, T. A. (2013). The multiple altimeter beam experimental Lidar (MABEL), an airborne simulator for the ICESat-2 mission. *Journal of Atmospheric and Oceanic Technology*, *30*(2), 345–352. https://doi.org/10.1175/JTECH-D-12-00076

Meredith, M., Sommerkorn, M., Cassotta, S., Derksen, C., Ekaykin, A., Hollowed, A., et al. (2019). Polar regions. In H.-O. Pörtner, D. C. Roberts, V. Masson-Delmotte, P. Zhai, M. Tignor, E. Poloczanska, et al. (Eds.), *IPCC special Report on the ocean and cryosphere in a changing climate*.

Morison, J., Hancock, D., Dickinson, S., Robbins, J., Roberts, L., Kwok, R., et al. (2020). Algorithm theoretical basis document (ATBD) for ocean surface height ICESat-2 scientific computing facility. https://doi.org/10.5067/F3KMPQD9663P

National Research Council. (2012). *Seasonal-to-decadal predictions of Arctic sea ice: Challenges and strategies.* The National Academies Press.

Neuenschwander, A., Popescu, S. C., Nelson, R. F., Harding, D., Pitts, K. L., & Robbins, J. (2020). Algorithm theoretical basis document (ATBD) for land-vegetation along-track products (ATL08). ICESat-2 Scientific Computing Facility. https://doi.org/10.5067/ATJ2993XY4MI

Neumann, T. A., Brenner, A., Hancock, D., Robbins, J., Saba, J., Harbeck, K., et al. (2020). *ATLAS/ICESat-2 L2A global geolocated photon data, version 3*. NASA National Snow and Ice Data Center Distributed Active Archive Center. https://doi.org/10.5067/ATLAS/ATL03.003

Neumann, T. A., Martino, A. J., Markus, T., Bae, S., Bock, M. R., Brenner, A.C., et al. (2019). The Ice, cloud and land elevation satellite-2 mission: A global geolocated photon product derived from the advanced topographic laser altimeter system. *Remote Sensing of Environment*, *233*. https://doi.org/10.1016/j.rse.2019.111325

Palm, S., Yang, Y., & Herzfeld, U. (2020). Algorithm theoretical basis document (ATBD) for atmosphere Part 1: Level 2 and 3 data products. ICESat-2 Scientific Computing Facility. https://doi.org/10.5067/XVKMH2X1HVJ1

Schutz, B. E., Zwally, H. J., Shuman, C. A., Hancock, D., & DiMarzio, J. P. (2005). Overview of the ICESat Mission. *Geophysical Research Letters*, *32*, L21S01. https://doi.org/10.1029/2005GL024009

Smith, B. (2018). Algorithm theoretical basis document (ATBD) for land ice along-track height product (ATL06). ICESat-2 Scientific Computing Facility. https://doi.org/10.5067/A8SP5FCJLWR0